Molecular electrostatics of $[V_{10}O_{28}]^{6-}$ cluster: a graphics visualization study using PARAM

Shridhar R. Gadre, Sangeeta V. Bapat, A. Taspa and Rajendra N. Shirsat

Department of Chemistry, University of Poona, Pune 411 007, India

The molecular electrostatic potential (MESP) maps of decavanadate $[V_{10}O_{28}]^{6-}$ ion are obtained using transputer-based parallel machine PARAM with an efficient algorithm. The graphics visualization package has been developed on an IRIS 4D/20 computer. The timings and MESP maps are compared with those due to Rohmer et al. (Rohmer, M-M., Ernenwein, R., Ulmschneider, M., Wiest, R. and Bénard, M., Int. J. Quant. Chem., 1991, 40, 723–744; Kempf, J.-Y., Rohmer, M-M., Poblet, J.-M., Bo, C. and Bénard, M., J. Am. Chem. Soc., 1992, 114, 1136–1146). The basicity of various oxygens is studied and it is seen that the deepest MESP minimum occurs around the oxygen bonded to three vanadium atoms. Some of the critical points (CPs) of MESP are located and characterized in terms of the eigenvalues of the respective Hessians. A further highlight of this work is the existence of a negative MESP region in the centre of the cluster.

MOLECULAR electrostatic potential (MESP) has been employed[1,2] as an important tool for the investigation of molecular reactivity. A variety of applications of this entity (MESP) are found in organic chemistry, pharmacology, biology, chemistry of explosives, drug designing, etc. Earlier[3,4] applications have focused on location of sites of electrophilic attack, viz. the negative valued minima that appear in the MESP maps. However, a recent work due to Sjoberg and Politzer[5] makes use of the MESP for prediction of nucleophilic attack as well.

The MESP $V(r)$ at a reference point r, due to a molecular electronic charge distribution $\rho(r)$, is given as

$$V(\mathbf{r}) = \sum_{A}^{N} Z_A/|\mathbf{r} - \mathbf{R}_A| - \int \rho(\mathbf{r}')d^3r'/|\mathbf{r} - \mathbf{r}'|$$

where N is the total number of nuclei in the molecule and Z_A is the charge of the nucleus at $\mathbf{R}_A$. The two terms in the above equation refer to the nuclear and electronic contribution respectively. Recently[6], we have developed an algorithm for the efficient computation of MESP maps from Gaussian based wavefunctions. This algorithm is based on rigorous bounds which are used for pre-emptive elimination of small contributions to MESP. A further efficient parallel version of this algorithm has been developed on a 64-node PARAM machine. This version utilizes the SHELL concept whereby the storage requirements are minimized. Excellent load-balancing is achieved since the (coarse-grain) parallelization is effected at the point-level. This

extends the use of our previously developed program[6] to large molecular systems. A good test ground for this purpose is offered by the $[V_{10}O_{28}]^{6-}$ cluster studied recently by Rohmer et al.[7a,b] as a benchmark for large molecular calculations. The CPU times reported by Rohmer et al.[7a] for MESP evaluation at 8034 and 5751 points (on $z = 0.0$ a.u. and $z = 3.47$ a.u. planes) are approximately 29 and 20 minutes respectively on a single CRAY-2 machine. In the present work, we have employed the MO wavefunction due to Rohmer et al.[7a] for MESP computations. With our novel algorithm enriched by elimination of numerically insignificant integrals, and the SHELL concept which helps in reduction of storage requirement, the typical time for 5427 MESP evaluations for double and single precision versions are 43 and 25 minutes respectively on a 64-node PARAM machine at C-DAC, Pune. It may be noted here that the typical rating of this cluster of 64 INMOS T800 based processors is estimated to be only 20 to 25 megaflops. The *distributed* memory available on this machine is restricted to 256 megabytes as compared to 2 gigabytes on the CRAY processor. It may, therefore, be concluded that our parallel algorithm enables us to achieve the performance of a single CRAY with our otherwise limited computational resources! Needless to say that porting of our algorithm to CRAY will indeed achieve a very superior performance.

The topography of the MESP of negative ions is of special interest as is shown by the recent works by Gadre et al.[8] They have proven that every anion carries a mantle of negative valued directional MESP minima around it. This has resulted[8] in a rigorous definition of size, shape and potential anisotropy of anions. Around each oxygen atom in the $[V_{10}O_{28}]^{6-}$ cluster, one also expects to find negative valued local minima corresponding to lone pairs. That it is indeed so can be found in figure 5 of ref. 7a. The estimate of sizes (a_x, a_y, a_z) of the decavanadate cluster may be obtained along the three cartesian axes. The value of a_x (X-axis contains four oxygen atoms in $z = 0$ plane) turns out to be 19.4 a.u. whereas the a_y and a_z values are 14.2 and 16.0 a.u. respectively. The color graphics visualization of the plane $z = 0$ is shown in the figure on the cover page of the journal. This visualization program was developed on a personal IRIS 4D/20 machine available at C-DAC, Pune. The special features of this program are: (i) almost equal distribution of three basic colours (RGB) and (ii) strategies for smoothing the pictures.

We have exploited in this work our previously described fast parallel algorithm along with this graphics visualization program to probe the reactivities at various sites of $[V_{10}O_{28}]^{6-}$ cluster. We have scanned a variety of planes for this purpose. Displayed in this work are a few representative samples in Figures 2 and 3. Figure 1 displays a typical view of this cluster. The relative sizes of V and O are only illustrative and

Figure 1. A typical view of ball and stick model of $[V_{10}O_{28}]^{6-}$ cluster.

are not quantitatively correct. The geometry of the cluster is described in detail in ref. 7. There are six vanadium and twelve oxygen atoms in the basal plane ($z = 0.0$ a. u.).

It may be seen from the MESP maps in Figures 2 and 3 and the one on the cover page that the minimum potential changes from (all coordinates and MESP values in a. u. in the subsequent discussion) -0.68 to -0.72 as one scans from $z = 0.0$ through $z = 5.2$ a. u. planes. The MESP minima in the planes $z = 0.0$ through

$z = 3.0$ are approximately constant (viz. $V = -0.682$ a. u.). These planes show the minimum located near the oxygen shared between two terminal vanadium atoms. However, the MESP minima get progressively lower thereafter. The site at which the potential is minimum is also shifted, as is seen from the figures. We notice that the most negative potential (-0.72013 a. u.) occurs at the point $(0.0, -4.15661, 4.703)$ in the vicinity of the oxygen atom bonded to three vanadiums. It subsequently increases with progressively increasing values of z. In this connection, it may be pointed out that Rhomer et al.[7a] reported the results for only two planes, viz. $z = 0.0$ and $z = 3.47$, and have found the lowest contour value of -0.699 in the latter. We have further located and characterized some of the critical points of MESP of this cluster (cf. Table 1). All the CPs have appropriate symmetry-related partners.

The values $\nabla^2 V$ and $4\pi\rho$ match at all the CPs in Table 1 up to 10 significant digits as predicted by the Poisson equation. Between the two minima in the mantle (as typified by CP 4) there is seen a chain of five saddles (typified by CP 8, CP 3, CP 2) of type $(3, +1)$ parallel to X-axis. Though this appears rather surprising, there is no contradiction since the extremal characteristics of these saddle points vary (cf. Table 1). A similar chain of saddles is observed parallel to the Y-axis but no minimum is observed along this direction in the mantle. Only two of these saddles (CP 5 and CP 7) are found and are reported in Table 1.

We notice another unique feature in the MESP distribution of this cluster, viz. the presence of negative valued 'hole' around the centre. Such a behaviour has not been exhibited (to the best of our knowledge) by
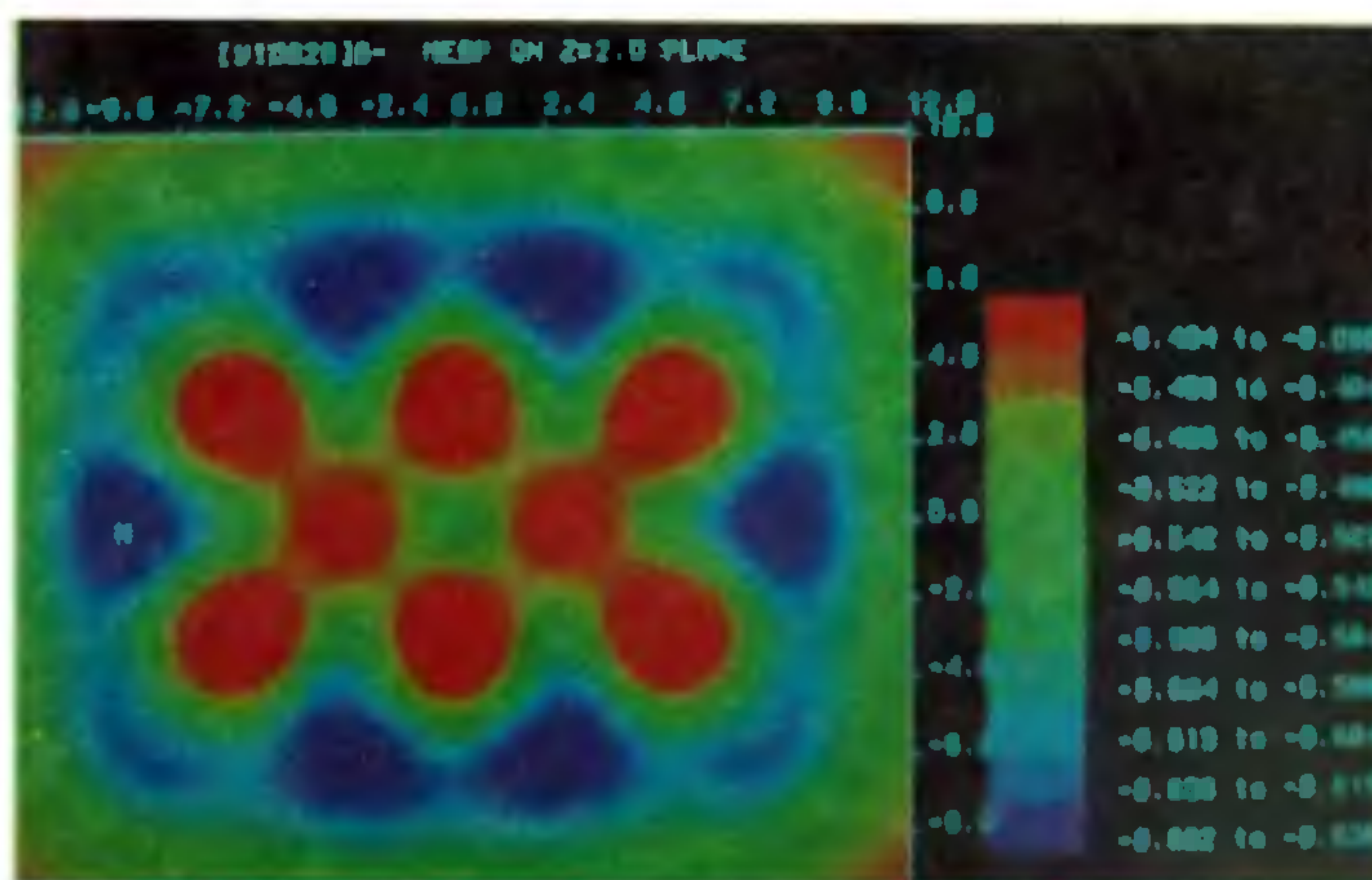

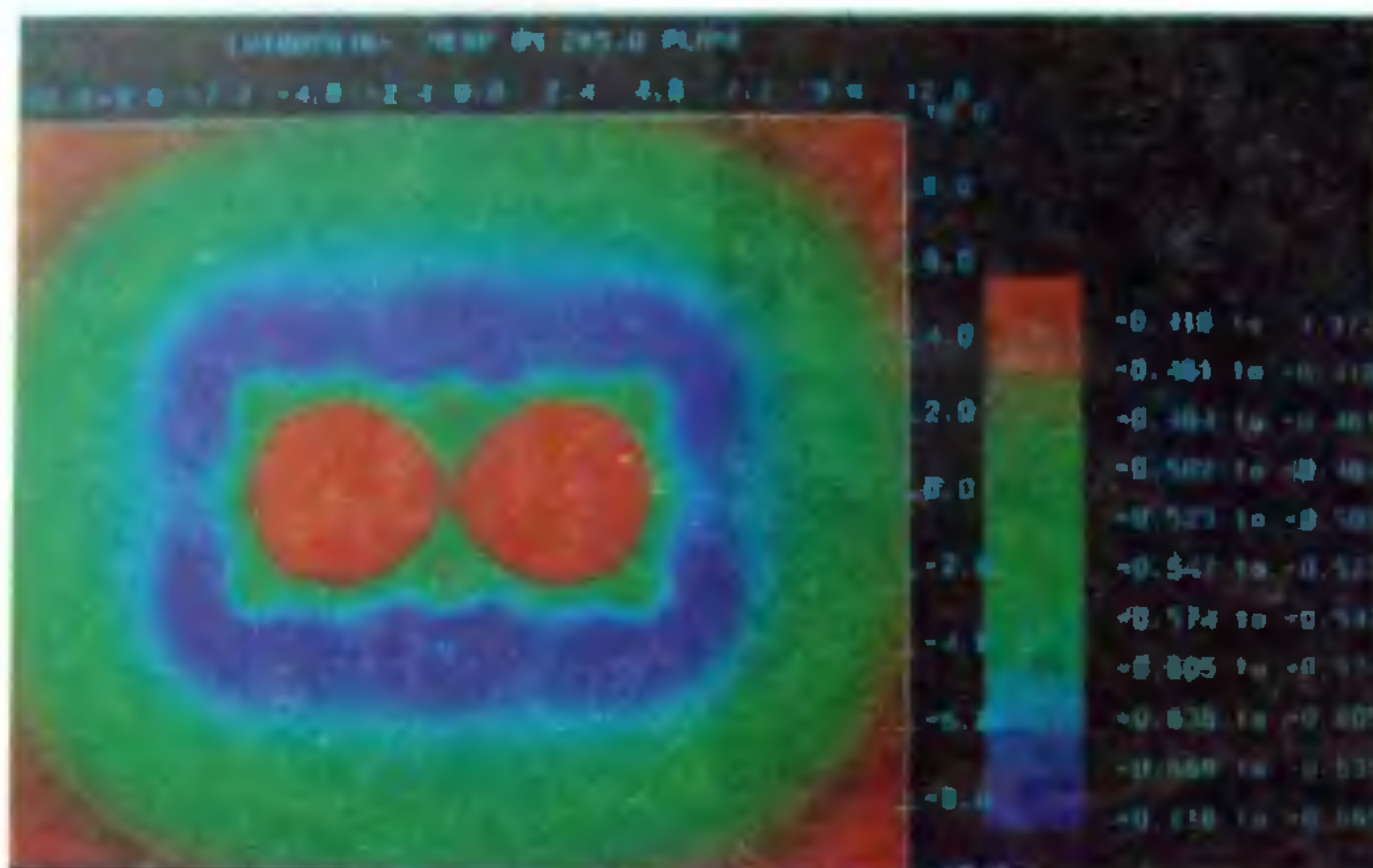Figure 2. MESP map of decavanadate ion in the plane $z = 2$ a. u.

Figure 3. MESP map of decavanadate ion in the plane $z = 5$ a.u

Table 1. Some critical points of MESP of $[V_{10}O_{28}]^6$ ion with their positions and characterization (all values in a.u)

CP	Coordinates x	y	z	Eigenvalues $\times 10^{-2}$			Nature	V(r)
1	0.00	−4.15	4.70	1.53.	26.0.	2.57	(3, +3)	−0.7201
2	0.00	7.08	0.00	−4.69.	8.26.	0.69	(3, +1)	−0.6352
3	2.26	7.18	0.00	1.35.	24.0.	−0.079	(3, +1)	−0.6723
4	6.68	7.14	0.00	1.40.	17.0.	0.092	(3, +3)	−0.6297
5	9.74	0.00	0.00	29.4.	1.91.	−0.089	(3, +1)	−0.6820
6	0.00	0.00	0.00	−0.08.	46.0.	−5.67	(3, −1)	−0.4867
7	9.92	4.14	0.00	18.5.	1.19.	−0.009	(3, +1)	−0.6217
8	5.53	6.95	0.00	−3.04.	8.26.	0.69	(3, +1)	−0.6240
9	0.00	0.00	7.99	−0.06.	1.47.	5.45	(3, +1)	−0.6817

any ring cage systems hitherto reported. This 'hole' extends to infinity along the z-direction providing a channel-like structure of negative MESP. A negative MESP 'hole' also exists between the two lateral vanadiums in the plane $z = 0$. The presence of these 'holes' could be attributed to the high degree of localization of electrons in the cluster, viz. 454 electrons are trapped inside a finite volume enclosed by the minimal surface[8] with $a_x = 19.4$, $a_y = 14.2$ and $a_z = 16.0$ a.u.

The Mulliken charge density for different types of atoms is studied and the values for oxygen are given in Figure 4. These values show that the oxygen atom (g) carries the maximum negative charge. This atom is surrounded by six vanadium atoms and is not available for protonation. The most basic oxygen shown by the MESP study is oxygen atom (c) in Figure 4 as discussed above. One expects this oxygen to be most negative as it is closer to three vanadium atoms and it is well outside the bulk. This oxygen has the charge density
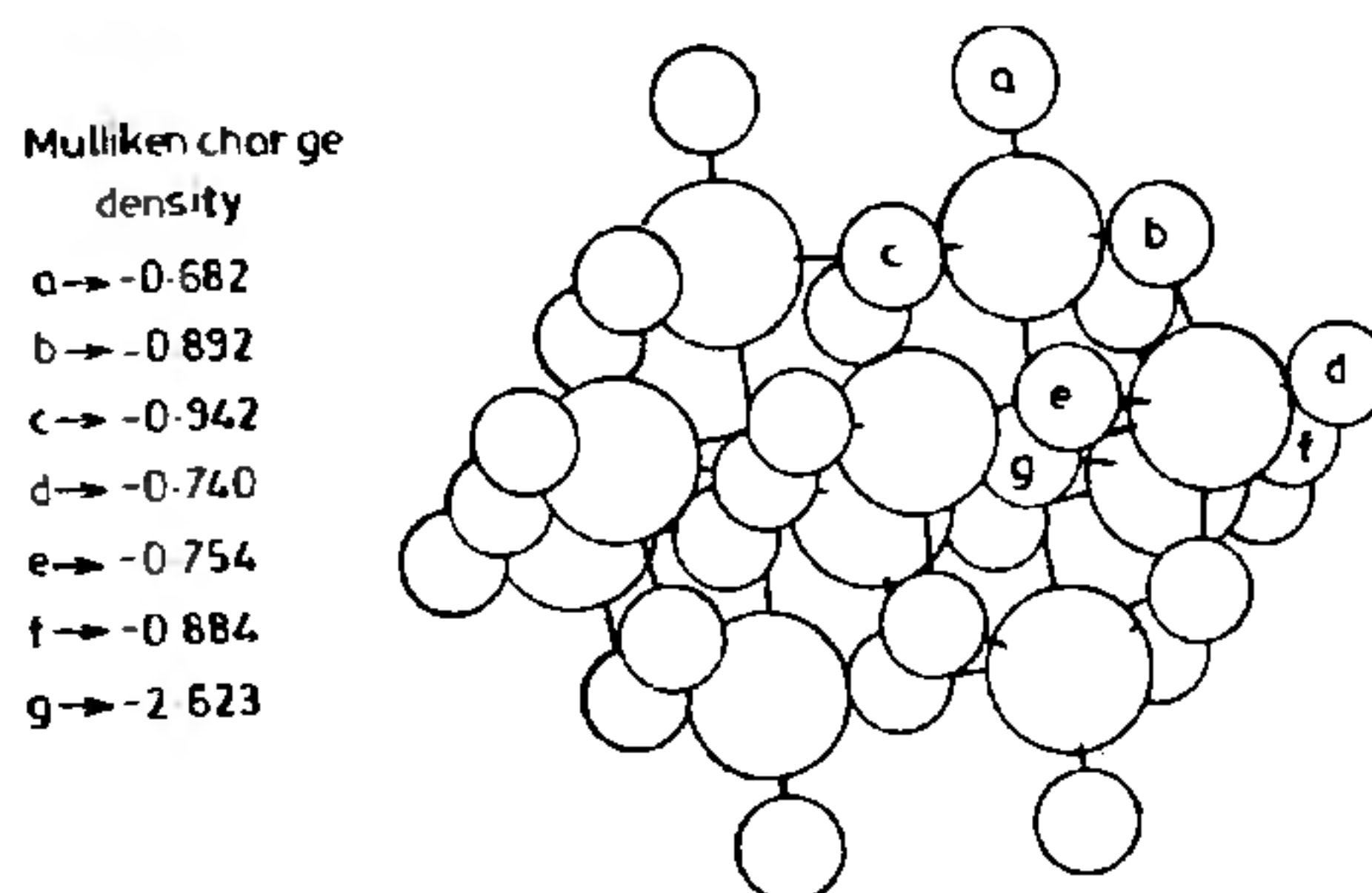
Mulliken charge density

a → −0.682
b → −0.892
c → −0.942
d → −0.740
e → −0.754
f → −0.884
g → −2.623

Figure 4. Mulliken populations for the decavanadate cluster.

value −0.94 a.u. and it is closer to the negative valued MESP mantle. The Mulliken charge density on oxygen decreases with the number of vanadium atoms closer to it. This conclusion is in agreement with the general

observation due to Pullman[1] that the basicity patterns revealed by Mulliken population analysis and those by MESP are not necessarily identical. After this analysis was done, we found that it has been reported by Kempf et al.[7b] Our values agree with those due to Kempf et al.[7b] to all the reported digits.

It is indeed gratifying that our efficient parallel algorithm fortified by graphics visualization can be usefully exploited for the study of basicity and topographical pattern around various atoms of large clusters.

1. See Pullman, B., Int. J. Quant. Chem.: Quant. Biol. Symp., 1990, 17, 81 for an excellent overview of applications of MESP to biology-related fields.
2. Tomasi, J., Bonaccorsi, R. and Cammi, R., in Theoretical Models of Chemical Bonding (ed. Maksić, R.), Springer, 1990, pp. 230–268.
3. Scrocco, E. and Tomasi, J., Adv. Quant. Chem., 1978, 11, 116.
4. Politzer, P. and Truhlar, D. G. eds., Chemical Applications of Atomic and Molecular Electrostatic Potential, Plenum, New York, 1981.
5. Sjoberg, P. and Politzer, P., J. Phys. Chem., 1990, 94, 3959.
6. Gadre, S. R., Bapat, S. V., Sundararajan, K. and Shrivastava, I. H., Chem. Phys. Lett., 1990, 175, 307; Gadre, S. R., Bapat, S. and Shrivastava, I. H., Comp. Chem., 1991, 15, 203.
7.a Rohmer, M.-M., Ernenwein, R., Ulmschneider, M., Wiest, R. and Bénard, M., Int. J. Quant. Chem., 1991, 40, 723.
7.b Kempf, J.-Y., Rohmer, M.-M., Poblet, J.-M., Carles, Bo. C and Bénard, M., J. Am. Chem. Soc., 1992, 114, 1136. This work came to our attention after the first version of this MS was submitted for publication.
8. Gadre, S. R., Kulkarni, S. A. and Shrivastava, I. H., J. Chem. Phys., 1992, 96, 5253; Gadre, S. R., Kölmer, C. and Shrivastava, I. H., Inorg. Chem., 1992 (in press); Gadre, S. R., Shrivastava, I. H., J. Chem. Phys., 1991, 94, 8384; Pathak, R. K. and Gadre, S. R., J. Chem. Phys., 1990, 93, 1770; Gadre, S. R. and Pathak, R. K., Proc. Indian Acad. Sci. (Chem. Sci.), 1990, 102, 18.

Uranium isotopes and radium in the Bhagirathi–Alaknanda river system: Evidence for high uranium mobilization in the Himalaya

M. M. Sarin, S. Krishnaswami, K. K. Sharma* and J. R. Trivedi
Physical Research Laboratory, Ahmedabad 380 009, India
*Wadia Institute of Himalayan Geology, Dehra Dun 248 001, India

Extensive measurements of dissolved ^{238}U and ^{226}Ra concentrations and [^{234}U/^{238}U] activity ratio have been made on samples collected from the Bhagirathi, Alaknanda and their tributaries—the source waters of the Ganga. The objectives of this study are to determine (i) the sources of U and Ra to the Ganga river; (ii) the weathering rate of uranium in the Himalaya, and (iii) the role of Himalayan–Tibetan rivers on the marine budget of uranium. The dissolved ^{238}U and ^{226}Ra concentrations in the Ganga source waters are typically $\sim 2\ \mu gl^{-1}$ and $\sim 0.2\ dpml^{-1}$ respectively. The low ^{226}Ra concentrations relative to ^{238}U in these waters indicate that Ra is far less mobile. The Bhagirathi and Alaknanda weather uranium from their drainage basins at a rate of $\sim 2\ kgkm^{-2}yr^{-1}$, comparable to that of the other Himalayan rivers like the Yamuna, Gandak and Ghaghara; but orders of magnitude higher than that derived for some of the world's major rivers (Amazon and Congo). These results suggest that large-scale mobilization of uranium in the Himalaya by rivers is ubiquitous. In the global context, the rivers draining the Himalayan–Tibetan region could be a major source of uranium to the oceans and that its supply via these rivers may have considerably influenced the marine budget of uranium.

ONE of the conspicuous characteristics of the Ganga river system is its high dissolved uranium concentration, $\sim 2\ \mu gl^{-1}$, compared to the global average concentration of $0.3\ \mu gl^{-1}$ in river waters[1,2]. The Ganga and the Brahmaputra, together, transport about 1000 tons of dissolved uranium to the estuaries of the Bay of Bengal annually[2]. Where does all this uranium come from? What is the relative contribution of uranium to the Ganga from the streams draining the high altitude Himalaya? What is the role of Himalayan rivers in the marine budget of uranium? To answer these questions, we have sampled the Ganga source waters—the Bhagirathi, the Alaknanda and their tributaries (Figure 1, a,b). The main lithological units drained by these rivers are the sedimentary and crystalline nappes[3,4]. The sedimentary units are made of carbonates, shales, slates and quartzites; whereas granites and gneisses are the primary constituents of the crystallines (Figure 1,a). For detailed lithological features of the drainage basin reference is made to Sarin et al.[5]. The Bhagirathi was sampled extensively from its source (at Gangotri) to its confluence with the Alaknanda at Devprayag (Figure 1,b). The two rivers merge with each other at Devprayag to form the Ganga.

Details of the sampling procedures have been described in Sarin et al.[2]. Briefly, uranium and radium isotopes were preconcentrated at site from ~ 20 litres of water within 24 h of collection. For uranium, water samples were filtered through 3-μm Gelman cartridge filters. The filtered water was acidified with nitric acid to pH ~ 1, spiked with ^{232}U and allowed to stand for ~ 6–8 h for equilibration. Uranium isotopes were extracted from water by coprecipitation with ferric